Check for updates

Chapter 2

Co-transcriptional Analysis of Self-Cleaving Ribozymes and Their Ligand Dependence

Luiz F. M. Passalacqua and Andrej Lupták

Abstract

Self-cleaving ribozymes are RNA molecules that catalyze a site-specific self-scission reaction. Analysis of self-cleavage is a crucial aspect of the biochemical study and understanding of these molecules. Here we describe a co-transcriptional assay that allows the analysis of self-cleaving ribozymes in different reaction conditions and in the presence of desired ligands and/or cofactors. Utilizing a standard T7 RNA polymerase in vitro transcription system under limiting Mg²⁺ concentration, followed by a 25-fold dilution of the reaction in desired conditions of self-cleavage (buffer, ions, ligands, pH, temperature, etc.) to halt the synthesis of new RNA molecules, allows the study of self-scission of these molecules without the need for purification or additional preparation steps, such as refolding procedures. Furthermore, because the transcripts are not denatured, this assay likely yields RNAs in conformations relevant to co-transcriptionally folded species in vivo.

Key words Ribozymes, Catalytic RNA, Self-cleaving ribozymes, Co-transcriptional analysis, Co-transcriptional kinetics, In vitro transcription, Metal-ion dependence, Ligand dependence

1 Introduction

Discovered over 30 years ago [1–5], self-cleaving ribozymes are catalytic RNA molecules that promote a site-specific self-scission reaction. The most common mechanism of the self-scission reaction is a general acid-base catalysis, where a transesterification involves a nucleophilic attack by a 2′-oxygen on the adjacent phosphodiester bond, producing a 2′ – 3′ cyclic phosphate and a 5-′-hydroxyl product [6–9], with metal ions and metabolites employed as potential cofactors [6, 7, 10, 11]. To date, nine self-cleaving ribozyme families have been discovered in nature, comprising the hammerhead [1, 2], hairpin [3], hepatitis delta virus (HDV) [4, 12], glucosamine-6-phosphate synthase (glmS) [11], Neurospora Varkud satellite (VS) [5], twister [13], twister sister (TS), pistol, and hatchet motifs [14].

Self-cleaving ribozymes are broadly distributed throughout all branches of life [13–16]. Likely involved in several roles in biology, some of the known functions include self-scission during rolling-circle replication of RNA genomes, co-transcriptional processing of retrotransposons, and metabolite-dependent gene expression regulation in bacteria [1, 2, 4, 5, 11, 17–25]. Recently, it has also been shown that metabolites may modulate the activity of self-scission of some ribozymes [26]. Genomic locations of these ribozymes suggest that they affect many other biological processes, some of which may not be directly associated with RNA scission. Other examples, including highly conserved mammalian ribozymes [27, 28], suggest that many new biological roles are yet to be discovered.

The discovery and understanding of self-cleaving ribozymes and their roles depend on the biochemical characterization of these molecules. An important aspect of this characterization is the kinetics investigation of self-scission under different conditions and in the presence of metabolites, cofactors, and other potential ligands, such as protein chaperones. The most common options in the investigation of the kinetics of ribozymes are the study of pre-purified ribozymes and the co-transcriptional self-cleavage analysis. The first method typically uses denaturing PAGE to fractionate transcripts of isolate uncleaved ribozymes, precipitation, and a refolding step, although less harsh conditions such as non-denaturing chromatography and precipitation-less concentration of the purified samples have been utilized [29]. A denaturing step is best avoided as refolding of the ribozymes can lead to conformations different from the co-transcriptional folding. This may happen when the RNA loses the directional order of folding (5' to 3') and the co-existence of different folding states is likely to increase. For example, a comparison of the co-transcriptional folding and Mg²⁺-initiated refolding after precipitation of the RNase P ribozyme revealed that even though all folding processes have kinetic traps and misfold, the Mg2+-initiated refolding involves residues in different regions of the molecule, while the co-transcriptional folding allows the 5' region to fold before the 3' region, eliminating major misfold traps [30]. Furthermore, it has been shown that the co-transcriptional folding notably enhances the self-scission of the human HDV-like ribozyme CPEB3 when compared to a pre-purified sample [31], and that self-cleavage transcripts of the HDV ribozyme with an attenuator in the 3' end could not be restored efficiently by renaturation [32]. Hence, the use of the co-transcriptional self-cleavage analysis is preferred when possible.

Standard co-transcriptional analysis relies on the study of the self-cleavage reaction in transcriptional buffer, while transcription occurs. This methodology is limited to the experimental conditions compatible with RNA polymerase activity. Additionally, the concurrent synthesis of new molecules of RNA has to be accounted for,

adding a second kinetic element to the analysis. Herein, we provide an alternative co-transcriptional assay that allows the analysis of selfcleaving ribozymes in different reaction conditions and in the presence of desired ligands. The in vitro transcription is performed under limiting amount of Mg²⁺, and the reaction is followed by a 25-fold dilution in desired condition of self-cleavage (buffer, ions, ligand, pH, temperature, etc.). The limiting amount of Mg²⁺ reduces the self-scission reaction during the initial transcription. Control experiments showed that a 25-fold dilution efficiently prevents any new RNA synthesis; therefore, our co-transcriptional kinetic analysis does not need to account for the kinetics of transcription, contrasting with the previously described analysis of co-transcriptional cleavage by Long and Uhlenbeck [33]. This method allows study of self-scission of these RNAs without the need of purification and a second kinetic parameter. This approach is also useful to synthetic biology, as self-cleaving ribozyme can be used as platforms to the development of new molecular biology tools, particularly gene expression-regulating aptazymes [34]. The method is also applicable to the study of other types of ribozymes, such as self-splicing introns [35, 36].

For the illustration of the methodology, we present an example of the HDV-like ribozyme drz-Fprau-1. Found in the human gut bacterium *Faecalibacterium prausnitzii*, the ribozyme cleavage site maps 106 nucleotides upstream of the phosphoglucosamine mutase (*glmM*) open reading frame [15]. The enzyme glmM catalyzes the transformation of glucosamine 6-phosphate (GlcN6P) into glucosamine 1-phosphate (GlcN1P) [37]. It was shown that GlcN6P, a natural metabolite, increases the self-scission rate of the ribozyme when compared to a no metabolite control [26].

2 Materials

Working with RNA requires care to avoid contamination by RNases. All solutions should be prepared using double-distilled RNase-free water (ddH₂O) and analytical grade reagents. All solutions should be tested for the presence of RNases before use. Chemicals and reagents are purchased from commercial suppliers. Radioactive [α -³²P] ATP should be handled and disposed with safety and according to current regulations of purchase, use, and disposal.

2.1 In Vitro Transcription

- 1. 10× transcription buffer: 400 mM Tris-HCl or HEPES pH 7.5, 100 mM DTT (dithiothreitol), 20 mM spermidine, 1% Triton X-100 (*see* **Notes 1** and **2**).
- 2. 100 mM MgCl₂ stock.
- 3. 25 mM stocks of each rGTP, rUTP, and rCTP.

- 4. 2.5 mM stock of rATP.
- 5. $\left[\alpha^{-32}P\right]$ rATP.
- 6. T7 RNA polymerase.
- 7. Purified stock of DNA template of the ribozyme to be studied with T7 promoter (*see* **Note 3**).

2.2 Self-Cleavage Assay

The cleavage buffer depends on the system to be studied and also on the experiment proposed. For the example illustrated here, a physiological-like buffer is used.

- 1. 2× self-cleavage buffer: 100 mM Tris-HCl or HEPES (pH 7.4), 20 mM NaCl, 280 mM KCl (see Note 4).
- 2. 100 mM MgCl₂ stock.
- 3. Stocks of the metabolite(s) of interest (if applicable).
- 4. 2× denaturing loading buffer: 8 M urea, 20 mM EDTA (*see* **Note 5**) (ethylenediaminetetraacetic acid), 0.05% (w/v) bromophenol blue, and 0.05% (w/v) xylene cyanol.

2.3 Denaturing Polyacrylamide Gel Electrophoresis (PAGE)

- 1. 40% bis-acrylamide 19:1.
- 2. Urea.
- 3. $10 \times$ TBE: 890 mM Tris-borate, 890 mM boric acid, 20 mM EDTA, pH 8.3.
- 4. TEMED (N,N,N',N'-tetramethylethylenediamine).
- 5. 10% (w/v) ammonium persulfate (APS).
- 6. Polyacrylamide gel solution: 8 M urea, $0.5 \times$ TBE, 15% bis-acrylamide 19:1 (store away from light).
- 7. Diluent gel solution: 8 M urea, $0.5 \times TBE$.
- 8. Set of small glass plates $(16.5 \times 22 \text{ cm})$ or medium glass plates $(16.5 \times 28 \text{ cm})$ for PAGE, 1.5- and 0.8-mm Teflon spacers, wide-toothed and narrow toothed combs to cast wells, cellulose chromatography paper, and plastic wrap.
- 9. Electrophoresis power supply.
- 10. Storage phosphor image screen.

3 Methods

3.1 In Vitro RNA Transcription Under Minimal Mg²⁺ Conditions

1. Prepare 100 μ L in vitro transcription mix by adding: 10 μ L of the 10× transcription buffer, 3.5 μ L of the 100 mM MgCl₂ stock, 4 μ L of the 25 mM stock of each rGTP, rUTP, and rCTP, 10 μ L of 2.5 mM stock of rATP, 1 μ L of [α -³²P] rATP, 1 unit of T7 RNA polymerase, complete volume to 90 μ L with ddH₂O. Note that 10% of the solution is accounted for the DNA template to be added in the next step. This mix can be saved

- at -20 °C prior to T7 RNA polymerase addition or at 4 °C after T7 RNA polymerase addition for later use. The goal of this step is to prepare an efficient transcription reaction under conditions with most of ${\rm Mg}^{2+}$ chelated by the rNTPs, leaving minimal ${\rm Mg}^{2+}$ to promote ribozyme catalysis.
- 2. Initiate transcription by adding 0.5 μ L of the DNA template with a T7 promoter of the ribozyme construct to be studied (~0.5 pmol) into 4.5 μ L of the in vitro transcription mix.
- 3. Incubate the reaction at 24 °C (room temperature) for 10 min, to initiate transcription (*see* **Note 6**).

3.2 Kinetics Assay

- 1. Prepare the self-cleavage mix by adding: $50~\mu L$ of the $2\times$ self-cleavage buffer, $5~\mu L$ of the $100~mM~MgCl_2$ stock, and desired concentration of any metabolite(s) if applicable. Complete volume to $96~\mu L$ with ddH_2O . Incubate at desired temperature of self-scission assay (see Note 7).
- 2. Set up a cone-bottom well-plate to aliquot time-point fractions and terminate reactions. Each well should contain 5 μ L of 2× denaturing loading buffer.
- 3. After 10 min of the in vitro transcription, withdraw a 1 μL aliquot of the reaction mixture, and terminate its transcription and self-scission by the addition of the 2× denaturing loading buffer. This is the zero time-point, used as reference for the kinetic analysis, showing the extent of the RNA production and self-scission that occurred during the transcription period. Control experiments showed that 10 min in vitro transcription is enough time to make sufficient ³²P-labeled RNA without significant self-scission catalysis.
- 4. Transfer the remaining 4.0 μ L volume of the transcription reaction into the pre-incubated 96 μ L of self-cleavage mix (25-fold dilution) and start timing the self-cleavage reaction under the new conditions. Collect aliquots of 5 μ L at the desired time-points, and terminate the self-scission by depositing the aliquots into the pre-prepared cone-bottom well-plate with 5 μ L of the 2× denaturing loading buffer.

3.3 Resolving the Results

Results are resolved using denaturing PAGE.

- 1. Prepare 50 mL of bis-acrylamide gel solution of the appropriate percentage for the RNA sample. For a 10% polyacrylamide gel solution, dilute the 15% bis-acrylamide gel stock solution with the diluent gel solution (*see* **Note 8**).
- 2. Wash the glass plates, 0.8 mm spacers, and small-tooth combs thoroughly with distilled water, then 70% ethanol solution. With bottom and side spacers properly placed, clip the plates together with clamps, making sure that there are no gaps between spacers in the bottom corners of the plates.

- 3. In a 15 mL tube, add 3 mL of the 15% bis-acrylamide gel solution. Add 20 μ L of TEMED and mix. To this, add 30 μ L of the 10% APS solution to initialize polymerization. Rapidly mix and pour into the gel plate assembly to create a plug at the bottom of the gel. Allow ~2 min for polymerization.
- 4. Once the plug is polymerized, to the 50~mL of the bis-acrylamide gel solution, add $50~\mu\text{L}$ of TEMED and mix. Next, add $500~\mu\text{L}$ of the 10% APS solution and mix to initialize polymerization. Pour into the gel plate assembly. Insert combs at desired depth and allow the gel to polymerize completely.
- 5. Take off clamps and carefully remove the combs and the bottom spacer. Move the assembly to an electrophoresis gel box. Add $0.5 \times$ TBE buffer to cover the top and bottom of the gel. Rinse the wells and the room left by the bottom spacer to remove air bubbles. Pre-run the gel at least for 30 min at 20 W (small plates) or 40 W (medium plates) before loading the samples (ideally, the gel has to be hot when touching for loading—this assures that the samples keep denatured during loading).
- 6. Turn off the power supply. Rinse the wells and load samples. Run the gel at 20 W (small plates) or 40 W (medium plates). The time of run may vary according to the length of the transcription product and fragments, and both dyes of the loading buffer can be used to estimate where the RNA products are in the gel. In general, a 40 min run is enough for constructs less than 110 nucleotides (see Note 9).
- 7. After the electrophoresis separation is done, turn off the power supply, remove the plate assembly, and uncast the set of plates carefully. Cover one side of the gel with cellulose chromatography paper (this removes excess liquid in the gel, preventing excessive sample diffusion during storage). Cover the entire gel in plastic wrap and expose it to a phosphor screen. Place the phosphor image screen cassette in a refrigerator during exposure (up to an overnight exposure). If a longer exposure is needed, the gel should be dried and then exposed to the phosphor image screen (see Notes 10 and 11).
- 8. Use a biomolecular imager system (like Typhoon series from GE Healthcare) to retrieve the gel image from the exposed phosphor image screen. Analyze the gel image by creating lane profiles of each lane and measuring band intensities using an appropriate software, such as ImageQuant (GE Healthcare) or Image J (Open source—NIH). For self-cleaving ribozymes, the single precursor RNA band (full length product) cleaves into two visible bands (5' and 3' products), which increases in intensity over time as the self-scission reaction is allowed to proceed.

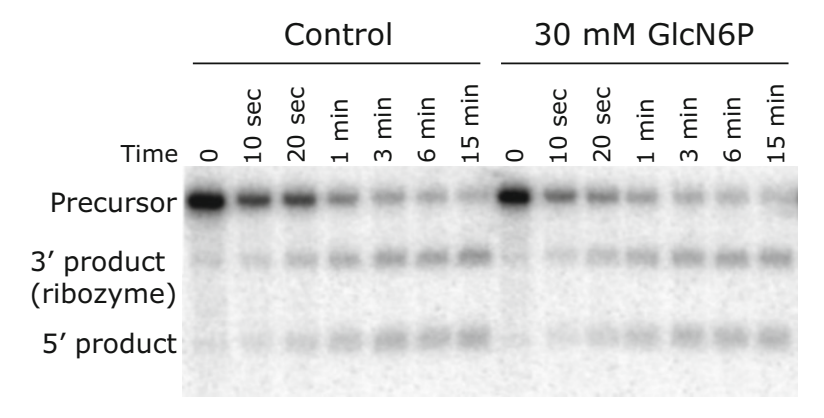


Fig. 1 Resolved denaturing (urea) PAGE gel of co-transcriptional self-scission of the drz-Fpra-1 ribozyme. In vitro co-transcriptional cleavage kinetics were performed in absence (control) and presence of 30 mM GlcN6P at a constant Mg^{2+} concentration (10 mM)

Figure 1 provides an illustration of a resolved gel image. In vitro co-transcriptional cleavage kinetics of drz-Fprau-1 were performed in presence and absence of GlcN6P.

3.4 Data Analysis

Several data-fitting software packages are currently available to perform data analysis. Herein, we explain how to analyze the data utilizing Microsoft Office Excel (MS Excel). We utilize linear least-squares optimization and the solver module of MS Excel to fit the data. The retrieved band intensities of the self-scission experiment are used to solve for the observed rates of self-cleavage ($k_{\rm obs}$) using linear regression analysis of a mono-exponential decay function, as shown below:

Fraction intact =
$$A \times e^{-kt} + C$$

where A and C represent the relative fractions of the ribozyme population cleaving with a rate constant k and remaining uncleaved population, respectively.

- In a MS Excel spreadsheet, horizontally, insert the band intensities values for each time-point, starting at column B. Leave column A for labeling the rows utilized: one for the single precursor RNA band, and two for the cleaved bands. Use row 1 to label and reference each lane from the gel.
- 2. In a convenient location on the spreadsheet, print arbitrary values corresponding to "A", "k", and "C" for the monoexponential decay and residuals model. For this example, the function and the cells used are: =\$K\$3*EXP(-\$L\$3*B8) + \$M\$3. Where \$K\$3 represents the value for "A", \$L\$3 represents the value for "k", B8 represents the time, and \$M\$3 represents the value for "C". The dollar sign ensures

- that the value in that cell is used regardless of where the formula is pasted in the spreadsheet. Therefore, the time value will change as the formula is pasted across the time-point columns. This programming is important for utilizing the "Solver" tool.
- 3. On the fifth row (=sum of bands), calculate the sum of the bands (precursor + cleaved ones).
- 4. On the sixth row (=time), insert the time-point for each aliquot withdrawn (use the same units for all time-points).
- 5. On the seventh row (=fraction), calculate the fraction of precursor RNA band (full length) for each time-point by dividing the value of the precursor band by the sum of the precursor and cleaved bands at a single time-point (= precursor band/sum of bands). The formula can be pasted into subsequent cells for each time-point without retyping.
- 6. On the eighth row (=model), as previously introduced, calculate the model for each time-point where "t" is the time and "A", "k", and "C" are arbitrary values for a mono-exponential decay model: =\$K\$3*EXP(-\$L\$3*B8) + \$M\$3. The formula can be pasted into subsequent cells for each time-point without retyping, because time is the variable that will change.
- 7. On the ninth row (=square difference), calculate the square of the difference at each time-point between the model value and the fraction cleaved [= (fraction model)²].
- 8. Calculate the sum of all square differences by programming using the SUM function in a new cell \$J\$11 (=sum of values of row 9).
- 9. Solver tool is an add-in which may need to be loaded into MS Excel via the Excel options and Add-ins tab menu. Solver is a tool for optimization and equation solving that finds the optimum value in one cell by adjusting the values in the cells the user specifies. Therefore, this tool can be used to solve the regression of the data points to the model, resulting in the $k_{\rm obs}$ value for the particular ribozyme.
 - (a) In MS Excel under the Data menu, select Solver in the Analyze subset.
 - (b) Set the target cell to the sum of the square differences by selecting the cell containing that value (\$J\$11).
 - (c) The goal is to minimize the value of that selected cell (sum of square differences), therefore, set "To:" to "min."
 - (d) "By changing variable cells": should be set to the arbitrary model values (A, k, C; \$K\$3-\$M\$3 in our example).
 - (e) Click "Solve". Allow the process to complete. The model value cell L\$3 should now contain the k_{obs} value for the particular ribozyme (the value for k).

- (f) The "Solve" processing can be visualized if both the calculated model values and the fraction cleaved values are plotted vs. time.
- 10. Alternatively, Solver tool is also available as an add-in for Google docs spreadsheet.

Figure 2 shows the MS Excel spreadsheet used for the data analysis of both kinetics experiments presented on Fig. 1.

4 Notes

- 1. Make all buffers in a $5 \times$ or $10 \times$ concentration to facilitate the preparation of the reactions. Store premade buffers at appropriate temperature.
- 2. The in vitro transcription buffer used usually cannot be the commercially available buffer supplied with the enzyme because of the high amounts of Mg²⁺. However, the rNTPs can be stretched to concentrations matching the Mg²⁺ concentration in the buffer to prevent significant ribozyme activity during the initial transcription reaction.
- 3. Do not forget to insert the T7 promoter sequence upstream of the DNA templates. To increase transcription yield, consider the sequence immediately downstream of the T7 RNA promoter. The +1 to +3 promoter sequence with nucleotides GGG or GGC affords the highest yield [38].
- 4. For conditions requiring a consistent ionic strength, the buffer and metabolite(s) stocks may have to be pH-adjusted by the addition of KOH or HCl. Additionally, the contribution of ions from the metabolite(s) stocks has to be tracked and considered in the final reaction composition. For example, glcN6P is typically available as sodium salt. Thus, titration of this metabolite has to be accounted for when determining the ionic strength.
- 5. Increase the EDTA concentration accordingly if reaction to be quenched has more than 10 mM Mg²⁺ and/or another divalent ion.
- 6. You can reduce the in vitro transcription temperature (down to 16 °C) to decrease the self-cleavage reaction during transcription. Note that the transcription yield will be reduced as well.
- 7. Use a thermocycler with a heated lid to avoid condensation of water on the lid of the tube. Solvent evaporation can drastically change the concentration of solutes.

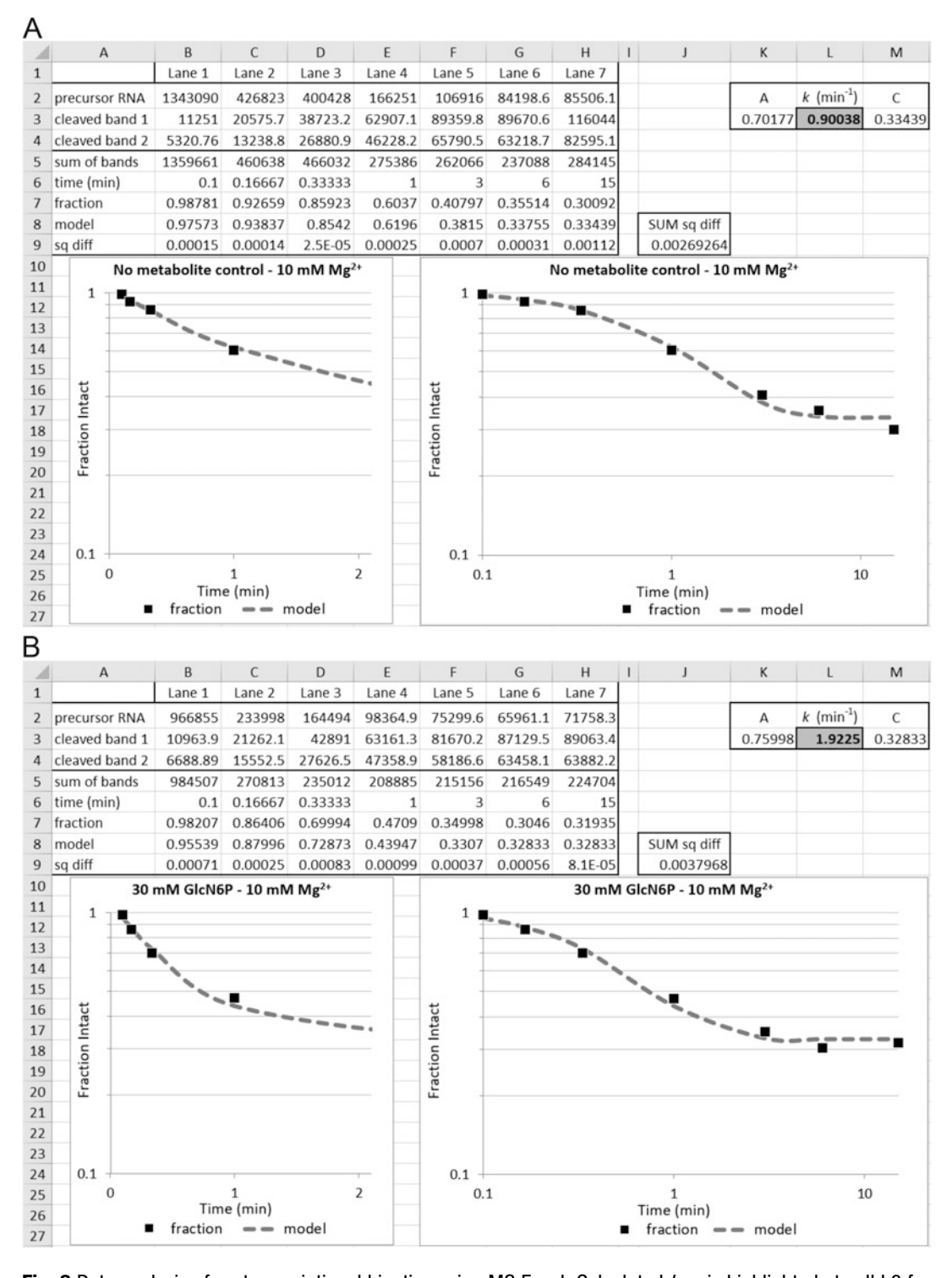


Fig. 2 Data analysis of co-transcriptional kinetics using MS Excel. Calculated $k_{\rm obs}$ is highlighted at cell L3 for both the no metabolite control (**a**) and the 30 mM GlcN6P experiments (**b**). Solver tool was used to find the best parameters to fit a simple monoexponential decay (A—fraction reacted, $k_{\rm obs}$ —self-scission rate constant) with an unreacted fraction (C) equation. The two graphs in each panel show identical data presented on log-linear (early time-points for visual comparison of initial self-scission rate) and log-log scales. The data derived from the PAGE images are shown with squares. The best-fit models are shown as dashed lines

- 8. Polyacrylamide gel percentage may differ according to the length of products and fragments generated by the self-scission reaction. In general, lower percentages of gels are used to have greater separation of fragments with similar lengths.
- 9. It is important to design constructs in a way that will allow the two product bands to be distinguishable by size separation.
- 10. Exposure time of the gel to the phosphor screen depends on the amount of ^{32}P -labeled material on the gel. To increase the labeling yield of $[\alpha^{-32}P]$ rATP, you may reduce the concentration of the non-radioactive rATP to 0.1 mM or even 0.05 mM in the in vitro transcription mix. Adjust the Mg^{2+} concentration accordingly.
- 11. ³²P is a high energy β-emitter. Avoid exposure to the radiation and radioactive contamination. Wear proper PPE to minimize exposure to radiation. Dispose of radioactive waste in accordance with the rules and regulations.

References

- 1. Prody GA, Bakos JT, Buzayan JM et al (1986) Autolytic processing of dimeric plant virus satellite RNA. Science 231:1577–1580
- 2. Hutchins CJ, Rathjen PD, Forster AC et al (1986) Self-cleavage of plus and minus RNA transcripts of avocado sunblotch viroid. Nucleic Acids Res 14:3627–3640
- 3. Buzayan JM, Gerlach WL, Bruening G (1986) Non-enzymatic cleavage and ligation of RNAs complementary to a plant virus satellite RNA. Nature 323:349–353
- 4. Sharmeen L, Kuo MY, Dinter-Gottlieb G et al (1988) Antigenomic RNA of human hepatitis delta virus can undergo self-cleavage. J Virol 62:2674–2679
- 5. Saville BJ, Collins RA (1990) A site-specific self-cleavage reaction performed by a novel RNA in neurospora mitochondria. Cell 61:685–696
- Jimenez RM, Polanco JA, Lupták A (2015) Chemistry and biology of self-cleaving ribozymes. Trends Biochem Sci 40:648–661
- Wilson TJ, Liu Y, Lilley DMJ (2016) Ribozymes and the mechanisms that underlie RNA catalysis. Front Chem Sci Eng 10:178–185
- 8. Ren A, Micura R, Patel DJ (2017) Structure-based mechanistic insights into catalysis by small self-cleaving ribozymes. Curr Opin Chem Biol 41:71–83
- 9. Seith DD, Bingaman JL, Veenis AJ et al (2018) Elucidation of catalytic strategies of small

- nucleolytic ribozymes from comparative analysis of active sites. ACS Catal 8:314–327
- Fedor MJ (2009) Comparative enzymology and structural biology of RNA self-cleavage. Annu Rev Biophys 38:271–299
- 11. Winkler WC, Nahvi A, Roth A et al (2004) Control of gene expression by a natural metabolite-responsive ribozyme. Nature 428:281–286
- 12. Wu HN, Lin YJ, Lin FP et al (1989) Human hepatitis delta virus RNA subfragments contain an autocleavage activity. Proc Natl Acad Sci 86:1831–1835
- Roth A, Weinberg Z, Chen AGY et al (2014) A widespread self-cleaving ribozyme class is revealed by bioinformatics. Nat Chem Biol 10:56–60
- 14. Weinberg Z, Kim PB, Chen TH et al (2015) New classes of self-cleaving ribozymes revealed by comparative genomics analysis. Nat Chem Biol 11:606–610
- 15. Webb CHT, Riccitelli NJ, Ruminski DJ et al (2009) Widespread occurrence of self-cleaving ribozymes. Science 326:953
- Hammann C, Luptak A, Perreault J et al (2012) The ubiquitous hammerhead ribozyme. RNA 18:871–885
- 17. Martick M, Horan LH, Noller HF et al (2008) A discontinuous hammerhead ribozyme embedded in a mammalian messenger RNA. Nature 454:899

- 18. Vazquez-Tello A, Rojas AA, Paquin B et al (2000) Hammerhead-mediated processing of satellite pDo500 family transcripts from *Doli-chopoda* cave crickets. Nucleic Acids Res 28:4037–4043
- 19. Ruminski DJ, Webb C-HT, Riccitelli NJ et al (2011) Processing and translation initiation of non-long terminal repeat retrotransposons by hepatitis delta virus (HDV)-like self-cleaving ribozymes. J Biol Chem 286:41286–41295
- 20. Eickbush DG, Eickbush TH (2010) R2 retrotransposons encode a self-cleaving ribozyme for processing from an rRNA cotranscript. Mol Cell Biol 30:3142–3150
- 21. Sánchez-Luque FJ, López MC, Macias F et al (2011) Identification of an hepatitis delta virus-like ribozyme at the mRNA 5'-end of the L1Tc retrotransposon from *Trypanosoma cruzi*. Nucleic Acids Res 39:8065–8077
- 22. Cervera A, De la Peña M (2014) Eukaryotic penelope-like retroelements encode hammerhead ribozyme motifs. Mol Biol Evol 31:2941–2947
- 23. Forster AC, Symons RH (1987) Self-cleavage of plus and minus RNAs of a virusoid and a structural model for the active sites. Cell 49:211–220
- 24. Epstein LM, Gall JG (1987) Transcripts of Newt satellite DNA self-cleave *in vitro*. Cold Spring Harb Symp Quant Biol 52:261–265
- 25. Ferbeyre G, Smith JM, Cedergren R (1998)

 Schistosome satellite DNA encodes active hammerhead ribozymes. Mol Cell Biol
 18:3880–3888
- 26. Passalacqua LFM, Jimenez RM, Fong JY et al (2017) Allosteric modulation of the Faecalibacterium prausnitzii hepatitis delta virus-like ribozyme by glucosamine 6-phosphate: the substrate of the adjacent gene product. Biochemistry 56:6006–6014
- 27. Salehi-Ashtiani K, Lupták A, Litovchick A et al (2006) A genomewide search for ribozymes reveals an HDV-like sequence in the human CPEB3 gene. Science 313:1788–1792

- 28. De la Peña M, García-Robles I (2010) Intronic hammerhead ribozymes are ultraconserved in the human genome. EMBO Rep 11:711–716
- Lupták A, Ferré-D'Amaré AR, Zhou K et al (2001) Direct pKa measurement of the activesite cytosine in a genomic hepatitis delta virus ribozyme. J Am Chem Soc 123:8447–8452
- 30. Pan T, Artsimovitch I, Fang X et al (1999) Folding of a large ribozyme during transcription and the effect of the elongation factor NusA. Proc Natl Acad Sci 96:9545–9550
- 31. Chadalavada DM, Gratton EA, Bevilacqua PC (2010) The human HDV-like CPEB3 ribozyme is intrinsically fast-reacting. Biochemistry 49:5321–5330
- 32. Diegelman-Parente A, Bevilacqua PC (2002) A mechanistic framework for co-transcriptional folding of the HDV genomic ribozyme in the presence of downstream sequence. J Mol Biol 324:1–16
- Long DM, Uhlenbeck OC (1994) Kinetic characterization of intramolecular and intermolecular hammerhead RNAs with stem II deletions. Proc Natl Acad Sci 91:6977–6981
- 34. Carothers JM, Goler JA, Juminaga D et al (2011) Model-driven engineering of RNA devices to quantitatively program gene expression. Science 334:1716–1719
- 35. Cech TR (1990) Self-splicing of group I introns. Annu Rev Biochem 59:543–568
- 36. Zhao C, Pyle AM (2017) Structural insights into the mechanism of group II intron splicing. Trends Biochem Sci 42:470–482
- 37. Mengin-lecreulx D, Van Heijenoort J (1996) Characterization of the essential gene *glmM* encoding phosphoglucosamine mutase in *Escherichia coli*. Mol Biol 271:32–39
- 38. Imburgio D, Rong M, Ma K et al (2000) Studies of promoter recognition and start site selection by T7 RNA polymerase using a comprehensive collection of promoter variants. Biochemistry 39:10419–10430